Carbohydrate Polymers 105 (2014) 135–144

Contents lists available at ScienceDirect

Carbohydrate Polymers

journal homepage: www.elsevier.com/locate/carbpol

Synthesis and characterization of a novel semi-IPN hydrogel based on Salecan and poly(N,N-dimethylacrylamide-co-2-hydroxyethyl methacrylate)

Xinyu Hu, Liandong Feng, Wei Wei, Aming Xie, Shiming Wang, Jianfa Zhang, Wei Dong*

Center for Molecular Metabolism, Nanjing University of Science & Technology, Nanjing 210094, China

ARTICLE INFO

Article history:
Received 29 August 2013
Received in revised form
22 November 2013
Accepted 18 January 2014
Available online 4 February 2014

Keywords:
Salecan
Poly(DMAA-co-HEMA)
Semi-IPN hydrogels
Porous structure
Robust materials

ABSTRACT

Salecan is a novel water-soluble, high molecular mass extracellular β-glucan produced by *Agrobacterium* sp. ZX09. Salecan has excellent physicochemical and biological properties, making it very suitable for hydrogel preparation. In this study, a series of novel semi-interpenetrating polymer network (semi-IPN) hydrogels containing Salecan and poly(N,N-dimethylacrylamide-co-2-hydroxyethylmethacrylate) (poly(DMAA-co-HEMA)) were synthesized by radical polymerization and semi-IPN technology. Structure and morphology of the hydrogels were characterized by FTIR, XRD, TGA and SEM. The semi-IPNs had a well-interconnected porous structure with tunable pore size ranging from 6 to 41 μm. Swelling capability of the hydrogels was improved by introducing the hydrophilic Salecan. Rheological results indicated that the incorporation of poly(DMAA-co-HEMA) into hydrogels enhanced the storage modulus. Compression tests revealed that these semi-IPNs were robust materials with compressive modulus between 13.3 and 90.5 kPa, the addition of Salecan increased the fracture strain from 71.1% to 88.8%. Degradation and cytotoxicity tests demonstrated that semi-IPNs were degradable and non-toxic.

1. Introduction

Hydrogel are hydrophilic three-dimensional polymeric networks that are able to absorb and retain a large quantity of water within their structure. Because of the characteristic properties of water in the hydrogels, they have been utilized in a wide range of applications, such as controlled drug delivery (Dumitriu, Oprea, & Vasile, 2009; El-Sherbiny, 2010), tissue engineering (Ma et al., 2010; Tang et al., 2010), column packing materials for chromatography (Gölgelioğlu, Bayraktar, Celebi, Uğuzdoğan, & Tuncel, 2012), wastewater treatment (Aouada, Pan, Orts, & Mattoso, 2009; El-Sherbiny, Abdel-Hamid, Rashad, Ali, & Azab, 2013) and agriculture (Bortolin et al., 2012). Hydrogels can be obtained by crosslinking of both natural and fully synthetic hydrophilic polymers. In general, hydrogels prepared from natural polymers such as polysaccharides offer great advantages, including excellent biocompatibility, biodegradability and low toxicity (Kulkarni, Mangond, Mutalik, & Sa, 2011; Shalviri, Liu, Abdekhodaie, & Wu, 2010). However, many of these polysaccharide-based hydrogels possess poor mechanical properties (Huang, Onyeri, Siewe, Moshfeghian, & Madihally, 2005). They are naturally brittle and cannot withstand the forces imposed in vivo, which restrict their widespread use in various biomedical applications. By contrast, hydrogels prepared from synthetic polymers usually present favorable mechanical properties, good processibility, easily tunable molecular weight and chemical compositions (Geng, Mo, Fan, Yin, & Fang, 2012; Yu & Ding, 2008). Unfortunately, most of them require relatively long response times for external environment change due to slow diffusion of water. Besides that, they may lack informational structure for biological response (Gil & Hudson, 2004; Tan & Marra, 2010). The fusion of polysaccharide and synthetic polymers in the form of (semi-) interpenetrating polymer network (IPN) hydrogels may offer to address these drawbacks and combine the most useful characters of both systems (Aouada, de Moura, da Silva, Muniz, & Mattoso, 2011; Dumitriu, Mitchell, & Vasile, 2011a,b; El-Sherbiny, Salama, & Sarhan, 2011).

Semi-IPN hydrogels are usually made by diffusing the linear polymer chains into a preformed polymer network, two polymers are independent of each other while being physically interlocked (Myung et al., 2008). In this way, the mechanical stability of the obtained hydrogels could be improved due to physical entanglements and network interactions (Bao, Yang, Mao, Mou, & Tang, 2008; Myung et al., 2008). Furthermore, semi-IPN hydrogels have interconnected porous network structures, which lead hydrogels to have much larger special surface areas (Zhao, Sun, Ling, & Zhou, 2009).

Salecan is a novel water-soluble extracellular β-glucan (Cas.No.1439905-58-4) produced by a new strain, *Agrobacterium* sp. ZX09. This strain was isolated from a soil sample from ocean coast of Shandong province (China) by our laboratory, its 16S rDNA

* Corresponding author. Tel.: +86 25 84318533; fax: +86 25 84318533.
E-mail address: dongwei@njust.edu.cn (W. Dong).

0144-8617/$ – see front matter © 2014 Elsevier Ltd. All rights reserved.
http://dx.doi.org/10.1016/j.carbpol.2014.01.051

sequence was deposited in the GenBank database under the accession number GU810841 (Xiu et al., 2010). The large scale production of Salecan is convenient, low cost and reproducible. Salecan is a linear (1→3)-β-D-glucan comprising β-1-3-linked glucopyranosyls with a small number of α-1-3-linked which was reported by our laboratory in 2010 (Xiu et al., 2010). As a novel microbial polysaccharides, Salecan has excellent biological activities including antioxidation and non-toxicity (edible safety). Our previous studies had shown that Salecan can be utilized in both the food and medical fields (Xiu et al., 2011; Xiu, Zhou, Zhu, Wang, & Zhang, 2011; Chen et al., 2011, 2012; Zhang et al., 2013; Zhou et al., 2013). Salecan also has unique physico-chemical properties. The molecular weight of Salecan is 2×10^6 Da and its solution has high viscosity, which represents good mechanical properties (Xiu et al., 2011; Xiu, Zhou, et al., 2011). In addition, Salecan contains a high density of hydroxyl groups, which can be modified to provide greater flexibility in the preparation of hydrogels. More importantly, the high solubility of Salecan allows large amounts of functional groups to be incorporated onto the polysaccharide chains without compromising its solubility in water. These features make Salecan a promising candidate for fabricating hydrogels used in different biotechnological applications.

Poly(N,N-dimethylacrylamide) (PDMA) is a hydrophilic polymer, due to its remarkable properties, such as water solubility and biocompatibility, it is very useful in the biomedical applications including polymer supports for protein synthesis, two-phase catalysts and controlled drug delivery (Kondo, Nakashima, Hado, & Tsuoa, 1990; Valdebenito & Encinas, 2010). Poly(2-hydroxyethyl methacrylate) (PHEMA), an important synthetic polymer, has been successfully applied in biomedical and pharmaceutical fields such as contact lenses, wound dressings and surgical prostheses because of their high mechanical strength, stability in water and inert to normal biological processes (Peppas, Hilt, Khademhossein, & Langer, 2006; Yildiz, Isik, & Kis, 2002). Copolymerization of HEMA monomers with other monomers has been reported by previous literature (Atzet, Curtin, Trinh, Bryant, & Ratner, 2008; Tomic, Dimitrijevic, Marinkovic, Najman, & Filipovic, 2009). The obtained copolymers present excellent biocompatibility and unique physicochemical properties (Peppas et al., 2006; La Gatta, Schiraldi, Esposito, D'Agostino, & De Rosa, 2009).

In this paper, a new class of semi-IPN hydrogels composed of Salecan and poly(DMAA-co-HEMA) (PDH) were prepared by radical copolymerization of DMAA and HEMA in the presence of Salecan and crosslinking agent N,N′-methylene diacrylamide (BAAm). To our knowledge, this is the first report on the preparation and characterization of Salecan/poly(DMAA-co-HEMA) semi-IPN hydrogels (Salecan/PDH semi-IPN hydrogels). The structure and interior morphology of the hydrogels were characterized by Fourier transformation infrared spectroscopy (FTIR), X-ray diffraction (XRD), thermogravimetric analysis (TGA) and scanning electron microscopy (SEM). The equilibrium swelling ratios, as well as the water retention capacity were measured as a function of time. The mechanical properties were investigated by rheological and compressive tests. Degradation tests were carried out in phosphate buffer saline (PBS) solution. Moreover, their cytocompatibility was assessed under in vitro conditions with COS-7 cell. Particularly, the effect of Salecan/PDH ratio on these properties of the resulting hydrogels were also studied.

2. Experimental

2.1. Materials

The 2×10^6 Da Salecan were made by Center for Molecular Metabolism, Nanjing University of Science & Technology. N,N-dimethylacrylamide (DMAA), 2-Hydroxyethyl methacrylate (HEMA), N,N′-methylene diacrylamide (BAAm), Ammonium persulfate (APS) and tetramethylethylenediamine (TEMED) were purchased from Aladdin Industrial Corporation. MTT cell proliferation and cytotoxicity detection kit was obtained from Nanjing KeyGen Biotech Co., LTD, China. The solutions of Salecan (2 wt%) were prepared by dispersing the required amount of Salecan in deionized water under slow stirring at room temperature overnight prior to assessment.

2.2. Preparation of Salecan/PDH semi-IPN hydrogels

Semi-IPN hydrogels based on Salecan and PDH were synthesized by free radical cross-linking copolymerization in aqueous solution at 25 °C. The preparation scheme is presented in Fig. 1. Briefly, 20 wt% monomer (DMAA + HEMA, DMAA/HEMA weight ratio = 1/1.5) solution containing 0.7 wt% crosslinking agent BAAm mixed with 2 wt% Salecan solution according to the desired blending ratios in 50 mL three-necked flask. Then the activator, TEMED was added and the solution was cooled to 0 °C in ice-water bath and stirred under Ar atmosphere for 1 h. After that, the initiator APS was added to the solution and stirred vigorously with mechanical stirrer for 180 s. Then 10 mL of this solution was transferred to a circular glass mold. The glass mold were sealed and placed in a thermostatted bath at 25 °C for 24 h. After polymerization, the samples were carefully removed from the mold and immersed in deionized water overnight. Then, these samples were further washed with a large excess of deionized water for 7 days, and the water was refreshed four times every day in order to remove the residual unreacted monomers and other impurities (Sarmad, Yenici, Gürkan, Keçeli, & Gürdağ, 2013). For all the cases, the washing solutions were collected and analyzed by the spectrophotometric technique to confirm the complete removal of the residual monomers (Dumitriu et al., 2011a,b). In addition, the feed composition and the samples code of the hydrogels are summarized in Table 1.

3. Characterization

3.1. Fourier transform infrared spectroscopy (FTIR)

The FTIR spectra were recorded in KBr pellets using a Nicolet IS-10 FTIR spectrometer in the region of 400–4000 cm^{-1}. Salecan, the freeze-dried PDH, SPDH2 and SPDH4 hydrogel samples were powdered, ground with KBr powder and pressed into pellets.

3.2. X-ray diffraction (XRD)

X-ray diffraction (XRD) measurements were conducted using a Philips PW 1720 X-ray generator operated at a voltage of 30 kV and 20 mA with CuKα radiation (λ = 0.154 nm) in the 2θ range of 0–60°.

3.3. Thermal-gravimetric analysis (TGA)

TGA analysis was conducted with a TA Model Q600 thermal gravimetric analyzer under a nitrogen atmosphere and at a heating rate of 10 °C/min in the temperature range of 0–600 °C.

3.4. Swelling behavior measurements

The preweighed dry hydrogels were immersed in deionized water at room temperature. At regular time intervals, the swollen hydrogels were taken out and weighed after wiping off the surface water with wet filter paper until a constant weight. The swelling ratio (SR) was determined according to the following equation:

$$SR = \frac{W_t - W_d}{W_d}$$

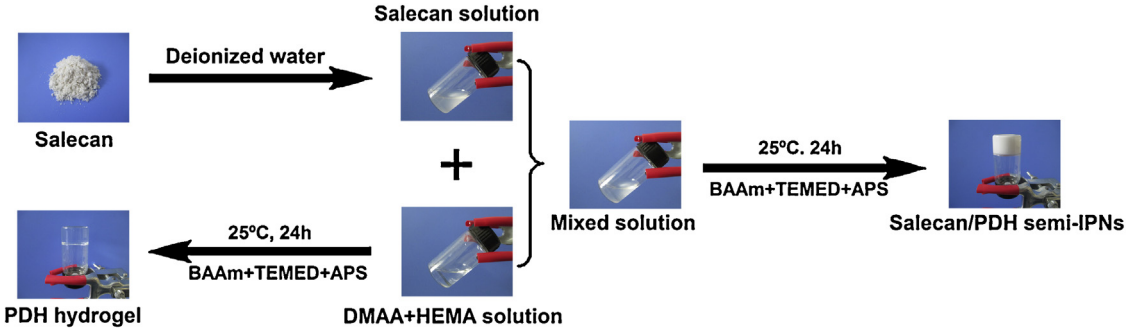

Fig. 1. Scheme showing the preparation of PDH and Salecan/PDH semi-IPN hydrogels.

Table 1
Composition of initial reaction mixtures used for the preparation of hydrogels.

Hydrogels	Salecan solution (2 wt%) (mL)	(DMAA + HEMA) solution (20 wt%) (mL)	TEMED (μL)	APS (mg)
SPDH1 (Sal/PDH = 80:20, v/v)	8	2	8	6
SPDH2 (Sal/PDH = 70:30, v/v)	7	3	12	9
SPDH3 (Sal/PDH = 60:40, v/v)	6	4	16	12
SPDH4 (Sal/PDH = 50:50, v/v)	5	5	20	15
PDH (Sal/PDH = 0:100, v/v)	0	10	40	30

Sal: Salecan, PDH: poly(N,N-dimethylacrylamide-co-2-hydroxyethyl methacrylate).

where W_t is the weight of the swollen hydrogel at time t and W_d is the weight of the dry hydrogel. The swelling kinetics in 0.9 wt% NaCl solution was tested in the same way.

The total water absorbed by the hydrogels at equilibrium was expressed as equilibrium water content (EWC), which was determined using the following equation:

$$\mathrm{EWC}(\%) = \frac{W_e - W_d}{W_e} \times 100$$

where W_e is the weight of the hydrogel at equilibrium. All results are obtained by averaging three measurements.

3.5. Water retention measurements

The dry hydrogel samples were first immersed in deionized water at room temperature till equilibrium. The equilibrium-swollen hydrogel samples were then quickly transferred into an oven at a temperature of 30 °C. The weight changes of hydrogels were recorded during the course of deswelling at predetermined time intervals. Water retention (WR) in the hydrogel was defined as:

$$\mathrm{WR}(\%) = \frac{W_t}{W_{eq}} \times 100$$

where W_t is the weight of hydrogel at time t during the shrinking process, and W_{eq} is the weight of the equilibrium-swollen hydrogel. All results are obtained by averaging three measurements.

3.6. Scanning electron microscopy (SEM)

The interior morphology of the porous hydrogels was observed by using a JEOLJSM-6380LV scanning electron microscope. Equilibrium swollen hydrogel samples were freeze-dried at −80 °C to completely remove water. After drying, these hydrogel samples were cut into thin slices and sputter-coated with gold to enhance conductivity.

3.7. Rheological measurement

Rheological measurements were carried out using an Anton Paar MCR101 rheometer with a parallel-plate geometry and a gap value of 1 mm. Dynamic frequency sweep experiments were performed at 0.5% strain in the range of 0.1–100 Hz (within the linear viscoelastic region as determined previously). The storage modulus (G') and loss modulus (G'') of the hydrogels were plotted as a function of frequency. All measurements were performed in duplicate at 25 °C.

3.8. Mechanical properties

Compression tests of the swollen hydrogels were performed on an Instron 4464 mechanical tester equipped with a 500 N load cell at room temperature. The cylindrical hydrogel samples (Ø24 mm × 10 mm) were tested at a compression rate of 2 mm/min. The compressive modulus was obtained by the initial (straight line) linear slope of the stress versus strain curve. Three parallel samples per measurement were performed, and the obtained values were averaged.

3.9. In vitro degradation

The degradation properties of the hydrogels were evaluated by incubating the hydrogels in phosphate buffer saline (PBS, pH 7.4) containing 0.02 wt% NaN_3 at 37 °C. The PBS solution was replaced every week throughout the study. At predetermined time intervals, the samples were removed from the solution, lyophilized and weighed. The weight remaining was calculated by using equation:

$$\text{Weight remaining}(\%) = \frac{W_t}{W_0} \times 100$$

where W_0 is the initial dry weight and W_t is the dry weight at time t. The experiment were conducted in triplicate.

3.10. Evaluation of cytotoxicity

Cytotoxicity tests of the hydrogel were carried out according to the guideline of international standard ISO 10993-5. The hydrogels were sterilized with 70% ethanol and then washed with sterile PBS. The extracts were prepared by immersing the sterilized hydrogels in Dulbecco's modified Eagle medium (DMEM) containing serum at 37 °C for 7 and 14 days, respectively. At the same time, COS-7 cells were incubated in a 96-well cell culture plate at a density of 10^3

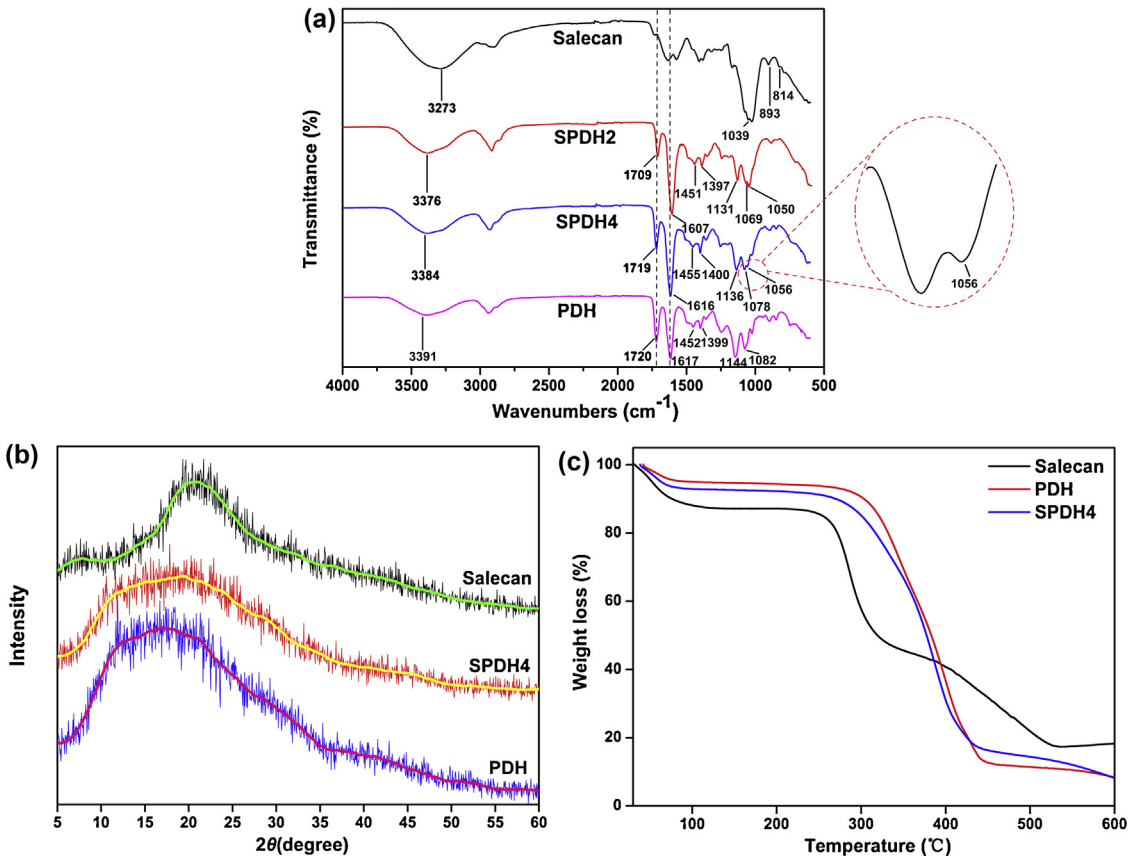

Fig. 2. FTIR spectra (a), XRD patterns (b) and TGA thermogram (c) of Salecan, PDH hydrogel and Salecan/PDH semi-IPN hydrogel.

cells per well in DMEM supplemented with 10% fetal bovine serum at 37 °C and 5% CO_2 for 24 h. After that, the culture medium was removed from the wells and replaced with the prepared extraction medium and incubated for another 24 h. Then 100 μl of MTT solution were added to each well and the cells were incubated at 37 °C for 4 h. 100 μl of dimethyl sulfoxide (DMSO) was then added to each well to dissolve the MTT formazan purple crystals. The optical density of the formazan solution was detected by an ELISA reader at 570 nm. In addition, fresh DMEM medium (without the hydrogel extracts) was used as a negative control. Data was calculated from the mean value of six parallel samples and the whole test was repeated three times.

4. Results and discussions

4.1. Preparation of hydrogels

Salecan/PDH semi-IPN hydrogels were synthesized by free radical copolymerization of DMAA and HEMA in the presence of Salecan using BAAm as crosslinker and APS/TEMED as initiator. The preparation scheme is given in Fig. 1. Similar preparations of other polysaccharide-based semi-IPN hydrogels have been previously described in the literature (Aouada et al., 2011; Dinu et al., 2011). During the polymerization reaction, the first step was a reaction between APS and TEMED. Briefly, the TEMED accelerated a homolytic scission on APS moieties to give sulfate free radicals (Feng, Guo, & Qiu, 1988), which initiated the copolymerization of DMAA, HEMA and BAAm in aqueous media. Finally, a three-dimensional network of PDH was formed and Salecan chains interpenetrated and become physically entangled within this PDH hydrogel network through hydrogen-bonding interaction.

4.2. FTIR analysis

The FTIR spectrum of Salecan/PDH semi-IPNs is reported in Fig. 2(a) and compared with those of Salecan and pure PDH hydrogel. In the case of Salecan, a broad band that appeared at 3273 cm^{-1} was attributed to the presence of O—H stretching vibrations. The peaks located at 1039 cm^{-1} assigned to the stretching vibrations of the C—OH bonds in glucopyranose ring. The presence of characteristic peak at 893 cm^{-1} confirmed that D-glucopyranose had a β-configuration. A weak characteristic absorption band at 814 cm^{-1} was due to the existence of a little α-glucopyranose (Xiu et al., 2010). For the pure PDH hydrogel, the strong absorption at 3391 cm^{-1} revealed the overlapping of the O—H stretching vibrations of PHEMA and N—H stretching vibrations (amide group) of BAAm (Madhusudana Rao et al., 2013). The strong peak at 1720 cm^{-1} was the characteristic stretching band for the ester carbonyl group (C=O) of PHEMA. The peaks at 1144 and 1082 cm^{-1} were associated with the stretching vibrations of C—O of the ester carbonyl group in PHEMA (Gils, Ray, & Sahoo, 2010). The main characteristic peaks of PDMAA appeared at 1617 cm^{-1}, which was assigned to the amide-I band of the amide group (tertiary amide). Two bands observed at 1452 and 1399 cm^{-1} represented the deformation vibration of $-CH_3$ group of PDMAA.

By considering Salecan/PDH semi-IPNs (Fig. 2a), new peaks appeared and the characteristic peaks for both Salecan and PDH were present with little shifting of position. Compared to the IR spectrum of PDH, SPDH4 showed a new peak at around 1056 cm^{-1}, corresponding to the C—OH stretching vibration of Salecan. Also, this peak can be seen at 1059 cm^{-1} in the spectrum of the physical mixture of Salecan and PDH (see Fig. S1 and Table S1 in Supporting Information). With increasing Salecan content in SPDH2,

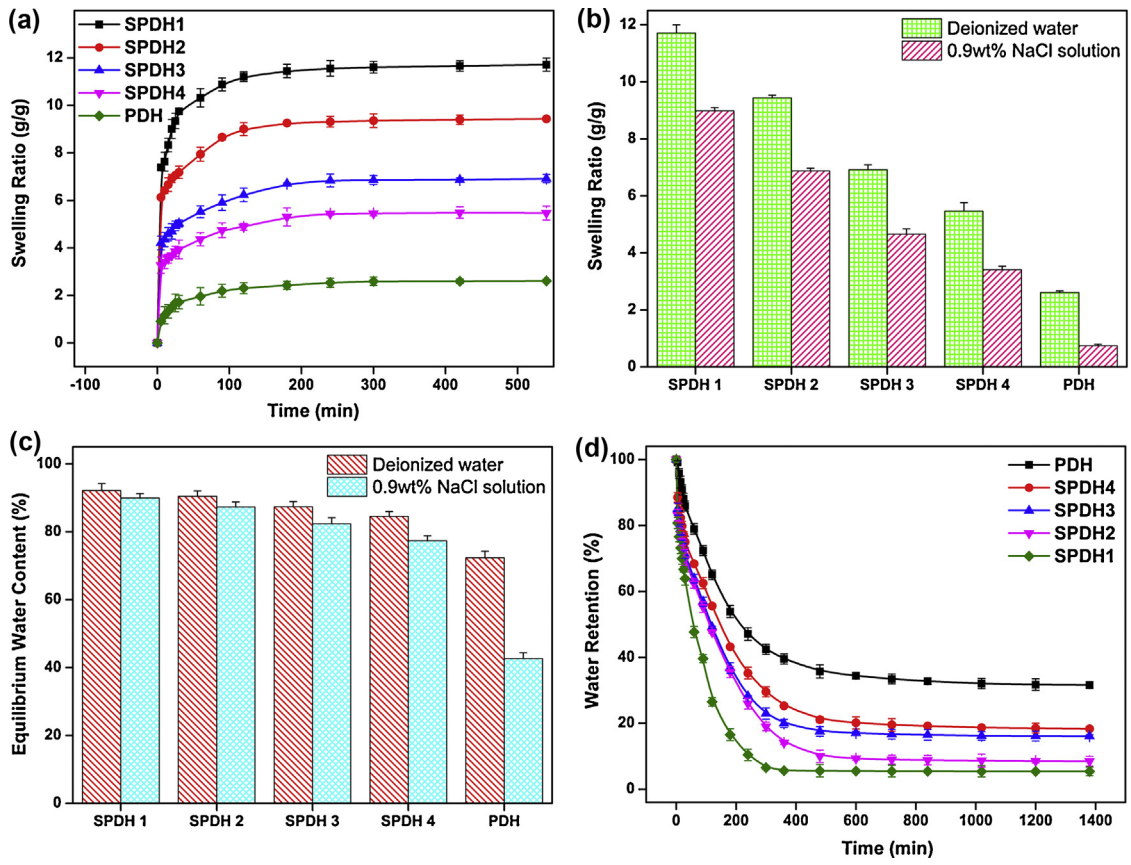

Fig. 3. Swelling kinetic curves in deionized water (a), swelling ratio values in deionized water and in 0.9 wt% NaCl solution (b), equilibrium water content (c) and water retention capacity (d) of PDH and semi-IPN hydrogels.

the characteristic absorption bands of Salecan at 1050 cm^{-1} was strengthened. These further confirmed the presence of Salecan in the semi-IPN hydrogels. Similar results were observed for other polysaccharide-based semi-IPN hydrogels (Li & Liu, 2008; Wen, Cao, Yin, Wang, & Zhao, 2009). Furthermore, the band at 3384 cm^{-1} in SPDH4 was attributed to the O—H stretching vibrations of PHEMA, which overlapped with the stretching vibrations of O—H (from Salecan) and N—H (from BAAm) to form a broad peak. The carbonyl absorption band of PHEMA and the amide-I band of the tertiary amide of PDMAA were observed at 1719 and 1616 cm^{-1}, respectively, in SPDH4. As the Salecan content increased, the absorption band of PHEMA was found to be shifted from 1720 cm^{-1}, in PDH, to 1709 cm^{-1}, in SPDH2. While the amide-I band of PDMAA experienced a shift from 1617 cm^{-1}, in PDH, to 1607 cm^{-1}, in SPDH2. These shifts suggested the formation of intermolecular hydrogen bonding between Salecan and PDH (Hernández & Mijangos, 2009; Lü, Liu, Ni, & Gao, 2010). In addition, other characteristic peaks of SPDH4 appeared at 1455 and 1400 cm^{-1} (—CH_3 deformation vibration) and at 1136 and 1078 cm^{-1} (C—O stretching vibrations of the ester carbonyl group), which were similar to the bands observed in PDH and SPDH2. From the FTIR results, it can be concluded that Salecan was incorporated into the hydrogel and the semi-IPN structure was formed, as already observed in the case of other semi-IPN hydrogels (Dragan et al., 2012; Li, Wen, Zhang, & Ju, 2013).

4.3. X-ray diffraction analysis

X-ray diffractogram of Salecan, SPDH4 and pure PDH are given in Fig. 2(b). The diffraction pattern of Salecan had a peak at $2\theta = 21^\circ$, corresponding to the crystalline regions of the polysaccharide structure. Compared to Salecan, SPDH4 displayed a weaker and broader peak at around $2\theta = 20^\circ$, indicating that the crystallinity of Salecan decreased with the presence of PDH. The incorporation of PDH polymer network in the semi-IPN hydrogels lead to the breaking of intra and inter-molecular hydrogen bonds of Salecan.

4.4. Thermal-gravimetric analysis (TGA)

Thermogravimetric degradation curves of Salecan, PDH and SPDH4 are displayed in Fig. 2(c). Salecan had a 12% weight loss at around 100 °C, which was ascribed to the loss of absorbed and bonded water. Subsequently, the weight loss about 55% was observed within the temperature of 250–350 °C, further a weight loss of 82% occurred at 350–575 °C. This may be attributed to the degradation of the main skeleton of Salecan. SPDH4 showed its thermal degradation in two stages. The first stage starting at room temperature and going up to 130 °C, with a small weight loss of 8%, corresponded to the elimination of water molecules trapped in the hydrogel. The second weight loss took place in the temperature range of 280–440 °C, and in this region the sample rapidly lost 83% of its weight. Beyond this, degradation of the sample continued up from 440 °C to 600 °C with a 94% weight loss. The results of the second and the third stage were caused by a series of complex process including dehydration of polysaccharide, depolymerization of poly(DMAA-co-HEMA) chains and decomposition of hydrogel networks into small molecules. From the TG curves, it can be concluded that the thermal stability of Salecan was improved upon by forming semi-interpenetrating networks of Salecan blended with poly(DMAA-co-HEMA).

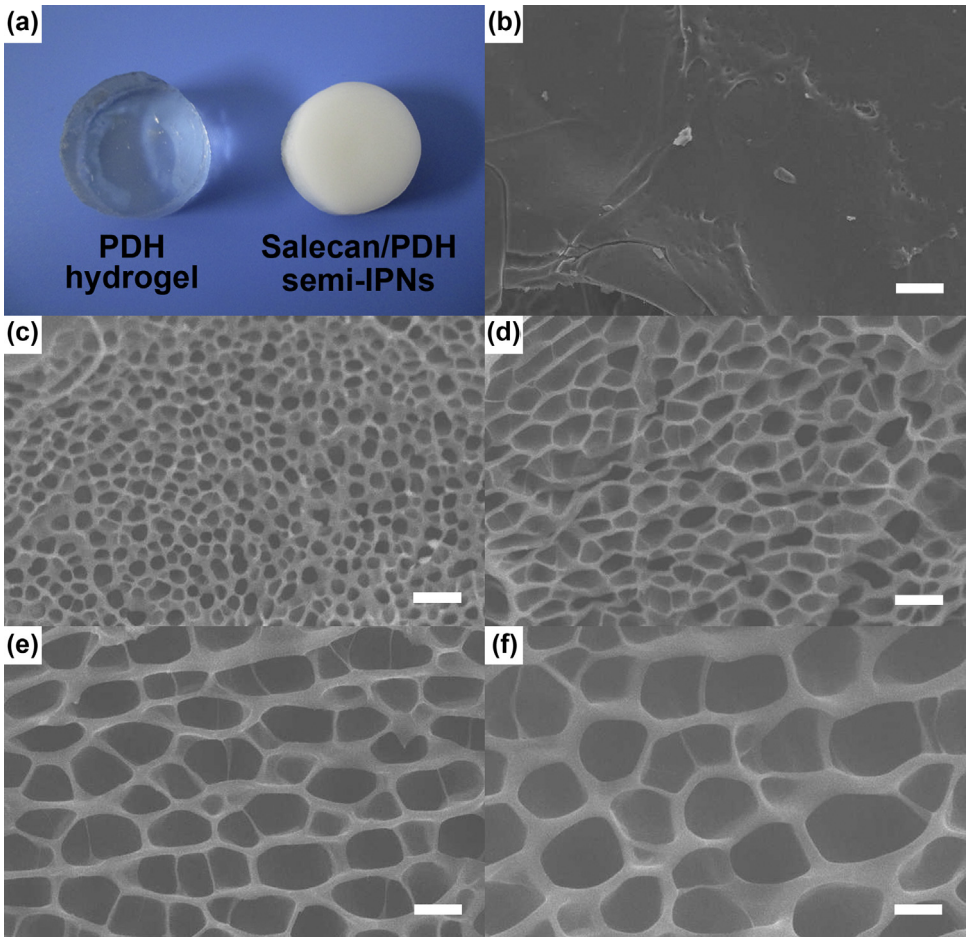

Fig. 4. Photograph (a) and SEM images (b–f) of PDH and semi-IPN hydrogels: (b) PDH hydrogel, (c) SPDH4, (d) SPDH3, (e) SPDH2, and (f) SPDH1. Scale bars represent 20 μm.

4.5. Swelling behavior test

Fig. 3(a) shows the swelling kinetic curves of the hydrogels in deionized water. It is clearly seen from Fig. 3(a) that the swelling ratio of the semi-IPNs increased as the Salecan/PDH ratio increased. SPDH1 showed a maximum swelling ratio of 11.7, compared to 2.6 in case of the pure SPDH. Generally, the swelling ratio is influenced by the overall hydrophilicity and the crosslinking density of the resulting hydrogel (Lopes & Felisberti, 2003). For the semi-IPN hydrogels, when the Salecan content increased, the hydrogel networks become more hydrophilic and consequently absorbed more water, resulting in an increased swelling ratio. Meanwhile, with the decrease in the PDH content, the crosslinking density of the hydrogels network decreased and molecular entanglement between Salecan and PDH was weakened, which lead to the improvement of the hydrogel swelling capacity. Conversely, the much higher crosslinking density of the pure PDH hydrogel significantly increased the friction between the polymeric chains and thus drastically decreased the available space for water in the swelling process (Bajpai & Giri, 2003; Dragan et al., 2012). Therefore, the lowest degree of swelling was observed.

Fig. 3(b) displays the equilibrium swelling ratio values of the hydrogels in deionized water and in 0.9 wt% NaCl solution. It can be found that the swelling ratios of the hydrogels in 0.9 wt% NaCl solution were lower than in deionized water. This is because that the increasing salt concentration decreased the osmotic pressure difference between gel network and external solution, which prevented water molecules to penetrate into the hydrogels.

In addition, the equilibrium water content (EWC) of the hydrogels was also studied (Fig. 3(c)). As it can be seen, all semi-IPN hydrogels exhibited EWC values greater than 80% in deionized water. In the case of the semi-IPNs, EWC values were observed to decrease slightly from about 92.1% to 84.5% with the decrease of the Salecan content. In contrast, the pure PDH hydrogel showed a minimum EWC value of about 72.3%. It is noted that the hydrogels showed a lower EWC in the presence of 0.9 wt% NaCl solution than in deionized water. This result further demonstrate that the ionic strength of a medium has a strong influence on the water absorbency of hydrogels.

4.6. Water retention test

The water retention capacity of all hydrogels are presented in Fig. 3(d). From the figure it was observed that as the PDH content increased, from SPDH1 to pure PDH hydrogel, the water retention capacity of the hydrogels were enhanced but the rate of water loss decreased. For instance, the water retention of the pure PDH hydrogel leveled off at about 31.6 wt% within 900 min, while that of SPDH1 leveled off at about 5.4 wt% within 420 min. The reason for this remarkable result is that the presence of more PDH in the hydrogels enhanced the crosslinking density of the network, which in turn hindered mobility and relaxation of the polymer chains, thus, the hydrogel became harder to lose water.

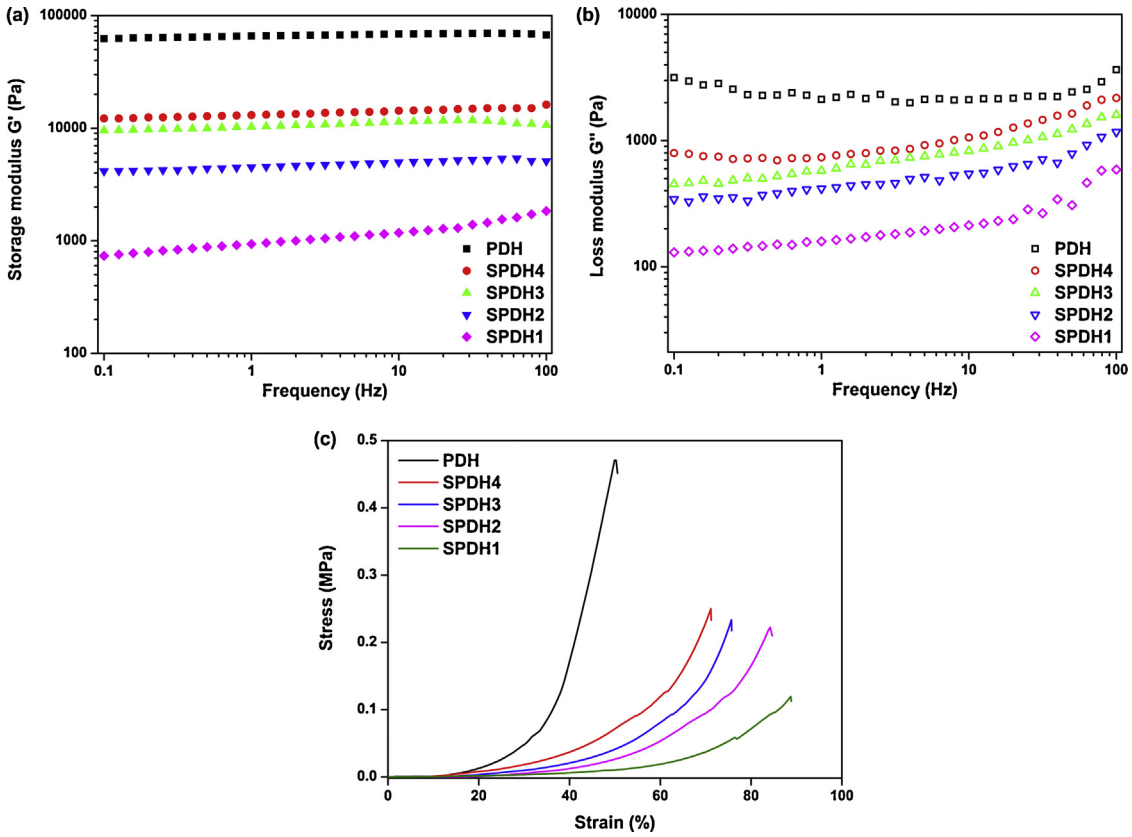

Fig. 5. Frequency dependence of (a) dynamic storage modulus, G' and (b) dynamic loss modulus, $G''$of PDH and semi-IPN hydrogels. (c) Typical stress–strain curves of PDH and semi-IPN hydrogels at room temperature.

4.7. SEM analysis

Fig. 4(a) depicts the photographs of the semi-IPN hydrogel (SPDH4) and the pure PDH hydrogel. The semi-IPN hydrogels were opaque and elastic, indicating a successful creation of this novel porous hydrogels composed of Salecan and synthesized PDH in the aqueous system. The interior morphologies of the freeze-dried PDH hydrogel and the semi-IPN hydrogels are shown in Fig. 4(b)–(f). The pure PDH hydrogel presented a continuous and even morphology without pores. In contrast, the semi-IPNs exhibited a highly interconnected porous structure with uniform pore distribution. It was observed that the average pore size of these semi-IPN hydrogels became smaller from SPDH1 to SPDH4. For example, SPDH1 had the largest pore size of approximately 41 ± 8 μm, while the pore size decreased to about 33 ± 10 μm, 16 ± 2 μm and 6 ± 1 μm in the case of SPDH2, SPDH3 and SPDH4 respectively. This trend may be related to the swelling ratio of the semi-IPN hydrogels discussed above. With the decrease of the Salecan/PDH ratio, the hydrophilic of the hydrogel network decreased and the crosslink density increased, which resulted in the decrease in water content and limited the water migration. Thus, the water was frozen into smaller ice nuclei in the lyophilization process. These ice nuclei were eventually represented by smaller pores (Li et al., 2001). This result also indicate that the pore size of the obtained semi-IPN hydrogels could be tailored by changing the composition ratio of Salecan/PDH.

4.8. Rheological study

The frequency sweep profiles of the storage modulus (G') and loss modulus (G'') were tested for the semi-IPN hydrogels and the pure PDH hydrogel, respectively (Fig. 5(a) and (b)). As can be observed, all the hydrogels showed typical gel rheological behavior. The G' values were greater than the G'' values for all the hydrogels throughout the entire frequency range of linear viscoelastic region, implying that the elastic behavior dominated over the viscous component (Chen, Chen, Bai, & Li, 2013). These features were characteristic of a strong gel with a network structure (Martnez-Ruvalcaba, Chornet, & Rodrigue, 2007). It can be seen that both the G' and G'' values of the semi-IPNs were significantly lower with respect to that of the pure PDH hydrogel. For all the semi-IPN hydrogels, both the G' and G'' values increased evidently when the PDH content increased, from SPDH1 to SPDH4. Generally speaking, the crosslinking density of polymer network and the flexibility of the polymer chains have a great influence on the rheological properties of the hydrogel. The introduction of more PDH chains inside of the semi-IPNs enhanced the density of polymer network and decreased the flexibility of chains due to the reinforced chain entanglements, resulting in an increase in the elastic modulus (Nie, Yuan, Zhao, Zhou, & Bao, 2013). It also demonstrated that the PDH content played a predominant role in the rheological properties of the semi-IPNs.

4.9. Mechanical properties

Fig. 5(c) displays the stress–strain curves of the semi-IPN hydrogels and the pure PDH hydrogel. The compressive modulus, fracture stress and fracture strain of the hydrogels are given in Table 2. Compared to the pure PDH, the semi-IPNs exhibited lower compressive modulus and stress. With increasing ratios of the PDH content from SPDH1 to SPDH4, the compressive modulus and stress of the semi-IPNs were improved correspondingly. The result indicated that semi-IPN hydrogels with higher PDH content possessed relatively dense and rigid networks, which was a considerable advantage that enables them to obtain higher modulus and to resist higher

Table 2
Compression properties of hydrogels at room temperature.

Hydrogels	Compressive modulus (kPa)	Fracture strain (%)	Fracture stress (kPa)
SPDH1	13.3 ± 1.8	88.8 ± 3.3	119.3 ± 2.4
SPDH2	29.5 ± 5.2	84.2 ± 2.5	222.1 ± 2.4
SPDH3	58.4 ± 8.0	75.7 ± 3.6	233.4 ± 3.0
SPDH4	90.5 ± 6.4	71.1 ± 1.7	250.0 ± 4.8
PDH	219.2 ± 4.3	49.9 ± 0.8	470.6 ± 10.3

stress. Most notably, the compressive modulus and stress of the semi-IPNs were consistent with their pore size. As mentioned earlier, SPDH4 exhibited a homogeneous porous structure with the smallest pores. This compact and uniformly structure contributed to distribute stress more evenly throughout the hydrogel surface (Kim et al., 2004). Meanwhile, the small pores played the efficient barrier role on the crack propagation. Thus, the compressive modulus and stress of SPDH4 were the highest among all the semi-IPNs. Conversely, SPDH1 had the largest pores, the loose network might result in the lowest compressive modulus and stress.

Although the pure PDH hydrogels showed the highest compressive modulus and stress, it broke at less than 50% of strain, while all the semi-IPN hydrogels did not break up to 70% of strain. The incorporation of more Salecan obviously increased the fracture strain of the semi-IPNs. In order to explain this, it should be considered that these fracture strain data were obtained from swollen hydrogels, the swelling behavior of the semi-IPNs had profound influence on their fracture strain. As noted above, an increase in the Salecan content helped bring about a higher swelling ratio and a looser network, thus, a large number of water molecules may easily move from the loading area to the unloading area in the deformation process, leading to a greatly enhanced fracture strain of the obtained hydrogel. Similar results can also be observed for the silk fibroin/polyacrylamide hydrogel system (Zaharia et al., 2012). On the other hand, Salecan had an important impact on the energy dissipation ability of the semi-IPNs due to its excellent viscosity properties. Salecan chains interdiffusing into the PDH network contributed to dissipate the deformation energy more efficiently. This effect prevented the hydrogel network from collapsing at a low strain. Obviously, Salecan/PDH semi-IPNs exhibited more favorable mechanical properties in comparison with the pure PDH hydrogel.

4.10. In vitro degradation

Fig. 6(a) shows the degradation profiles of the different hydrogels. After 9 weeks of incubation, the degradation of SPDH1 was the fastest with a remaining weight of about 55%. For SPDH2, SPDH3 and SPDH4, the weight remaining ratio was 61.8%, 67% and 70.6% respectively. Whereas the pure PDH only lost 12% of their original weight in 63 days degradation, which suggested that PDH hydrogel was very stable when immersed in PBS. The obvious weight loss of the semi-IPN hydrogels might be due to the diffusion of Salecan out of its semi-interpenetrating network (IPN) with PDH. The results also indicated that the crosslinking density played an important role in the degradation process. For example, SPDH1, which possessed the lowest cross-linking density, underwent surface erosion and degraded the fastest among the four semi-IPN hydrogel samples, while SPDH4 with the highest cross-linking density degraded at the slowest rate due to the lowest water accessibility.

4.11. Evaluation of cytotoxicity

Fig. 6(b) illustrates the viability of COS-7 cell cultured with the hydrogel extracts. As shown in Fig. 6(b), no statistically significant difference in cell viability was seen between the Salecan/PDH semi-IPN hydrogel extracts and negative control group after incubation

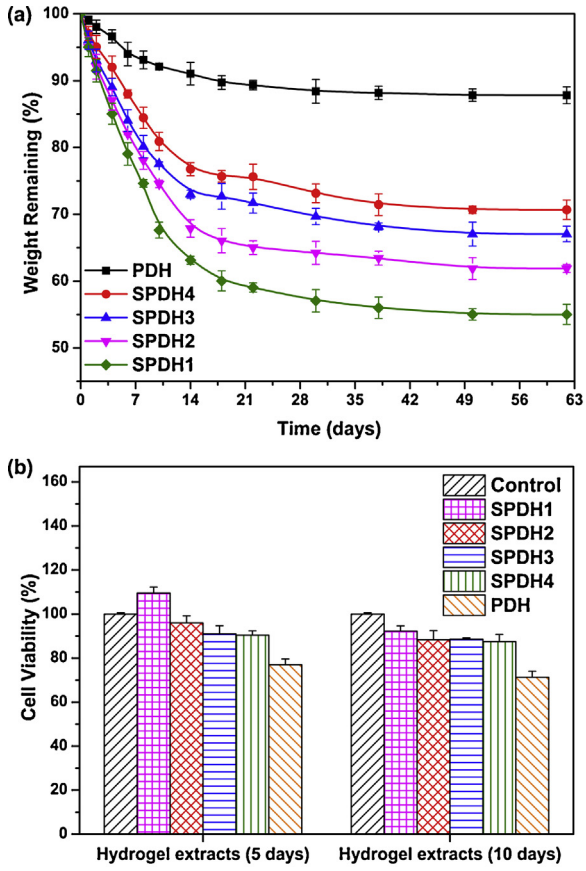

Fig. 6. Degradation (a) and cytotoxicity test (b) of PDH and semi-IPN hydrogels.

for 24 h. The excellent cytocompatibility of these semi-IPN hydrogels was ascribed to the biocompatibility of Salecan and the PDH hydrogel. The 5-day extract medium of SPDH1 showed a higher cell viability in comparison with the negative control group. This indicated that the 5-day extract medium of SPDH1 promoted the growth of COS-7 cell due to the edibility of Salecan dropping from the semi-IPNs during extraction (David-Raoudi et al., 2008). Furthermore, cells grown in different hydrogel extracts (5-days and 10-day) showed similar growth profiles. On the whole, the cell viability for all the semi-IPN hydrogels was greater than 85%. It can be inferred from these results that Salecan/PDH semi-IPN hydrogels are non-cytotoxic to COS-7 cell.

5. Conclusion

In this study, a new class of semi-IPN hydrogel was developed by incorporation of Salecan into a high strength copolymer network of poly(DMAA-co-HEMA). As a novel microbial polysaccharide, Salecan displayed its advantage for the design of hydrogels. In summary, the resulting semi-IPNs possessed desirable interior morphology, notable swelling ratio, favorable thermal stability and good mechanical properties. More importantly, these properties can be fine-tuned by varying the composition ratio of Salecan to PDH. The SEM investigations showed that the addition of Salecan into the PDH hydrogel achieved substantial changes in the final morphology. In comparison to the pure PDH hydrogel, semi-IPNs exhibited an uniformly distributed porous structure with internal diameter in the range of 6–41 μm. The swelling behavior and the water retention were dependent on the extent of cross-linking, as well as the hydrophilicity of the hydrogel network. With the decrease of the Salecan/PDH ratio, the swelling ratios and the rate of water loss decreased dramatically. The semi-IPN hydrogels

had remarkable EWC values compared with that of poly(DMAA-co-HEMA) hydrogel due to the existence of hydrophilic Salecan. Furthermore, rheological measurements showed that storage modulus G' increased with the increase of poly(DMAA-co-HEMA) content. The compressive modulus of the semi-IPNs were related to both the density of the polymer network and their pore size. The highest compressive modulus can even reach 90.5 kPa for SPDH4. While the fracture strain of the semi-IPNs was strongly influenced by the Salecan content and their swelling performance. SPDH1 can be compressed up to about 90% strain. Increasing the content of high-viscous Salecan could effectively dissipate the deformation energy. Finally, the cytotoxicity and degradability studies demonstrated that the semi-IPNs were non-toxic and degradable.

Acknowledgments

This work was supported by National Natural Science Foundation of China under the Grant 30870625 and the Fundamental Research Funds for the Central Universities, NUST2011XQTR07.

Appendix A. Supplementary data

Supplementary data associated with this article can be found, in the online version, at http://dx.doi.org/10.1016/j.carbpol.2014.01.051.

References

Aouada, F. A., Pan, Z., Orts, W. J., & Mattoso, L. H. C. (2009). Removal of paraquat pesticide from aqueous solutions using a novel adsorbent material based on polyacrylamide and methylcellulose hydrogels. *Journal of Applied Polymer Science*, *114*, 2139–2148.

Aouada, F. A., de Moura, M. R., da Silva, W. T. L., Muniz, E. C., & Mattoso, L. H. C. (2011). Preparation and characterization of hydrophilic spectroscopic, and kinetic properties of hydrogels based on polyacrylamide and methylcellulose polysaccharide. *Journal of Applied Polymer Science*, *120*, 3004–3013.

Atzet, S., Curtin, S., Trinh, P., Bryant, S., & Ratner, B. (2008). Degradable poly(2-hydroxyethyl methacrylate)-co-polycaprolactone hydrogels for tissue engineering scaffolds. *Biomacromolecules*, *9*, 3370–3377.

Bajpai, A. K., & Giri, A. (2003). Water sorption behaviour of highly swelling (carboxymethyl cellulose-g-polyacrylamide) hydrogels and release of potassium nitrate as agrochemical. *Carbohydrate Polymers*, *53*, 271–279.

Bao, L., Yang, W., Mao, X., Mou, S., & Tang, S. (2008). Agar/collagen membrane as skin dressing for wounds. *Biomedical Materials*, *3*, 044108.

Bortolin, A., Aouada, F. A., de Moura, M. R., Ribeiro, C., Longo, E., & Mattoso, L. H. C. (2012). Application of polysaccharide hydrogels in adsorption and controlled-extended release of fertilizers processes. *Journal of Applied Polymer Science*, *123*, 2291–2298.

Chen, P., Wang, Z., Zeng, L., Yang, X., Wang, S., Dong, W., et al. (2011). A novel soluble beta-glucan salecan protects against acute alcohol-induced hepatotoxicity in mice. *Bioscience Biotechnology and Bochemistry*, *75*(10), 1990–1993.

Chen, P., Wang, Z., Zeng, L., Wang, S., Dong, W., Jia, A., et al. (2012). Protective effects of Salecan against carbon tetrachloride-induced acute liver injury in mice. *Journal of Applied Toxicology*, *32*, 796–803.

Chen, Y., Chen, L., Bai, H., & Li, L. (2013). Graphene oxide–chitosan composite hydrogels as broad-spectrum adsorbents for water purification. *Journal of Materials Chemistry A*, *1*, 1992–2001.

David-Raoudi, M., Tranchepain, F., Deschrevel, B., Vincent, J. C., Bogdanowicz, P., Boumediene, K., et al. (2008). Differential effects of hyaluronan and its fragments on fibroblasts: Relation to wound healing. *Wound Repair and Regeneration*, *16*, 274–287.

Dinu, M. V., Perju, M. M., & Dragan, E. S. (2011). Porous semi-interpenetrating hydrogel networks based on dextran and polyacrylamide with superfast responsiveness. *Macromolecular Chemistry and Physics*, *212*, 240–251.

Dragan, E. S., Perju, M. M., & Dinu, M. V. (2012). Preparation and characterization of IPN composite hydrogels based on polyacrylamide and chitosan and their interaction with ionic dyes. *Carbohydrate Polymers*, *88*, 270–281.

Dumitriu, R. P., Oprea, A. M., & Vasile, C. (2009). A drug delivery system based on stimuli-responsive alginate/N-isopropylacryl amide hydrogel. *Cellulose Chemistry and Technology*, *43*, 251–262.

Dumitriu, R. P., Mitchell, G. R., & Vasile, C. (2011a). Multi-responsive hydrogels based on N-isopropylacrylamide and sodium alginate. *Polymer International*, *60*, 222–233.

Dumitriu, R. P., Mitchell, G. R., & Vasile, C. (2011b). Rheological and thermal behaviour of poly(N-isopropylacrylamide)/alginagte smart polymeric networks. *Polymer International*, *60*, 1398–1407.

El-Sherbiny, I. M. (2010). Enhanced pH-responsive carrier system based on alginate and chemically modified carboxymethyl chitosan for oral delivery of protein drugs: Preparation and in-vitro assessment. *Carbohydrate Polymers*, *80*, 1125–1136.

El-Sherbiny, I., Salama, M., & Sarhan, A. A. A. (2011). Ionotropically cross-linked pH-sensitive IPN hydrogel matrices as potential carriers for intestine-specific oral delivery of protein drugs. *Drug Development and Industrial Pharmacy*, *37*, 121–130.

El-Sherbiny, I., Abdel-Hamid, M., Rashad, M. I., Ali, M., & Azab, A. S. M. Y. A. (2013). New calcareous soil–alginate composites for efficient uptake of Fe(III), Mn(II) and As(V) from water. *Carbohydrate Polymers*, *96*, 450–459.

Feng, X., Guo, X., & Qiu, K. (1988). Study of the initiation mechanism of the vinyl polymerization with the system persulfate/N,N,N′,N′-tetramethylethylenediamine. *Die Makromolekulare Chemie*, *189*, 77–83.

Geng, X., Mo, X., Fan, L., Yin, A., & Fang, J. (2012). Hierarchically designed injectable hydrogel from oxidized dextran, amino gelatin and 4-arm poly(ethylene glycol)-acrylate for tissue engineering application. *Journal of Materials Chemistry*, *22*, 25130–25139.

Gil, E. S., & Hudson, S. A. (2004). Stimuli-responsive polymers and their bioconjugates. *Progress in Polymer Science*, *29*, 1173–1222.

Gils, P. S., Ray, D., & Sahoo, P. K. (2010). Designing of silver nanoparticles in gumarabic based semi-IPN hydrogel. *International Journal of Biological Macromolecules*, *46*, 237–244.

Gölgelioğlu, C., Bayraktar, A., Celebi, B., Uğuzdoğan, E., & Tuncel, A. (2012). Aqueous size exclusion chromatography in semimicro and micro-columns by newly synthesized monodisperse macroporous hydrophilic beads as a stationary phase. *Journal of Chromatography A*, *1224*, 43–50.

Hernández, R., & Mijangos, C. (2009). In situ synthesis of magnetic iron oxide nanoparticles in thermally responsive alginate- poly(N-isopropylacrylamide) semi-interpenetrating polymer networks. *Macromolecular Rapid Communications*, *30*, 176–181.

Huang, Y., Onyeri, S., Siewe, M., Moshfeghian, A., & Madihally, S. V. (2005). In vitro characterization of chitosan-gelatin scaffolds for tissue engineering. *Biomaterials*, *26*, 7616–7627.

Kim, U. J., Park, J., Li, C., Jin, H. J., Valluzzi, R., & Kaplan, D. L. (2004). Structure and properties of silk hydrogels. *Biomacromolecules*, *5*, 786–792.

Kondo, S., Nakashima, N., Hado, H., & Tsuoa, K. (1990). Poly(N,N-dimethylacrylamide-co-styrene)s as highly efficient catalysts for two-phase reactions. *Journal of Polymer Science Part A: Polymer Chemistry*, *28*, 2229–2232.

Kulkarni, R. V., Mangond, B. S., Mutalik, S., & Sa, B. (2011). Interpenetrating polymer network microsphere of gellan gum and egg albumin entapped with diltiazem-resin complex for controlled release application. *Carbohydrate Polymers*, *83*, 1001–1007.

La Gatta, A., Schiraldi, C., Esposito, A., D'Agostino, A., & De Rosa, A. (2009). Novel poly(HEMA-co-METAC)/alginate semi-interpenetrating hydrogels for biomedical applications: synthesis and characterization. *Journal of Biomedical Materials Research Part A*, *90A*, 292–302.

Li, G., Wen, Q., Zhang, T., & Ju, Y. (2013). Synthesis and properties of silver nanoparticles in chitosan-based thermosensitive semi-interpenetrating hydrogels. *Journal of Applied Polymer Science*, *127*, 2690–2697.

Li, M., Wu, Z., Zhang, C., Lu, S., Yan, H., Huang, D., et al. (2001). Study on porous silk fibroin materials. II. Preparation and characteristics of spongy porous silk fibroin materials. *Journal of Applied Polymer Science*, *79*, 2192–2199.

Li, S., & Liu, X. (2008). Synthesis, characterization and evaluation of semi-IPN hydrogels consisted of poly(methacrylic acid) and guar gum for colon-specific drug. delivery. *Polymers for Advanced Technologies*, *19*, 371–376.

Lopes, C. M. A., & Felisberti, M. I. (2003). Mechanical behaviour and biocompatibility of poly(1-vinyl-2-pyrrolidinone)-gelatin IPN hydrogels. *Biomaterials*, *24*, 1279–1284.

Lü, S., Liu, M., Ni, B., & Gao, C. (2010). A novel pH- and thermo-sensitive PVP/CMC semi-IPN hydrogel: swelling, phase behaviour, and drug release study. *Journal of Polymer Science Part B: Polymer Physics*, *48*, 1749–1756.

Ma, G., Yang, D., Li, Q., Wang, K., Chen, B., Kennedy, J. F., et al. (2010). Injectable hydrogels based on chitosan derivative/polyethylene glycol dimethacrylate/N,N-dimethylacrylamide as bone tissue engineering matrix. *Carbohydrate Polymers*, *79*, 620–627.

Madhusudana Rao, K., Mallikarjuna, B., Krishna Rao, K. S. V., Sudhakar, K., Chowdoji Rao, K., & Subha, M. C. S. (2013). Synthesis and characterization of pH sensitive poly(hydroxyethyl methacrylate-co-acrylamidoglycolic acid) based hydrogels for controlled release studies of 5-fluorouracil. *International Journal of Polymeric Materials and Polymeric Biomaterials*, *62*, 565–571.

Martnez-Ruvalcaba, A., Chornet, E., & Rodrigue, D. (2007). Viscoelastic properties of dispersed chitosan/xanthan hydrogels. *Carbohydrate Polymers*, *67*, 586–595.

Myung, D., Waters, D., Wiseman, M., Duhamel, P. E., Noolandi, J., & Ta, C. N. (2008). Progress in the development of interpenetrating polymer network hydrogels. *Polymers for Advanced Technologies*, *19*, 647–657.

Nie, W., Yuan, X., Zhao, J., Zhou, Y., & Bao, H. (2013). Rapidly in situ forming chitosan/ε-polylysine hydrogels for adhesive sealants and hemostatic material. *Carbohydrate Polymers*, *96*, 342–348.

Peppas, N. A., Hilt, J. Z., Khademhossein, A., & Langer, R. (2006). Hydrogels in biology and medicine: from molecular principles to bionanotechnology. *Advanced Materials*, *18*, 1345–1360.

Sarmad, S., Yenici, G., Gürkan, K., Keçeli, G., & Gürdağ, G. (2013). Electric field responsive chitosan–poly(N,N-dimethyl acrylamide) semi-IPN gel films and

their dielectric, thermal and swelling characterization. *Smart Materials and Structures*, *22*, 055010.

Shalviri, A., Liu, Q., Abdekhodaie, M. J., & Wu, X. Y. (2010). Novel modified starch–xanthan gum hydrogels for controlled drug delivery: Synthesis and characterization. *Carbohydrate Polymers*, *79*(4), 898–907.

Tan, H., & Marra, K. G. (2010). Injectable, biodegradable hydrogels for tissue engineering applications. *Materials*, *3*, 1746–1767.

Tang, Y., Wang, X., Li, Y., Lei, M., Du, Y., Kennedy, J. F., et al. (2010). Production and characterization of novel injectable chitosan/methylcellulose/salt blend hydrogels with potential application as tissue engineering scaffolds. *Carbohydrate Polymers*, *82*, 833–841.

Tomic, S. L., Dimitrijevic, S. I., Marinkovic, A. D., Najman, S., & Filipovic, J. M. (2009). Synthesis and characterization of poly(2-hydroxyethyl methacrylate/itaconic acid) copolymeric hydrogels. *Polymer Bulletin*, *63*, 837–851.

Valdebenito, A., & Encinas, M. V. (2010). Effect of solvent on the free radical polymerization of N,N-dimethylacrylamide. *Polymer International*, *59*, 1246–1251.

Wen, X., Cao, X. L., Yin, Z. H., Wang, T., & Zhao, C. S. (2009). Preparation and characterization of konjac glucomannan–poly(acrylic acid) IPN hydrogels for controlled release. *Carbohydrate Polymers*, *78*, 193–198.

Xiu, A. H., Kong, Y., Zhou, M. Y., Zhu, B., Wang, S. M., & Zhang, J. F. (2010). The chemical and digestive properties of a soluble glucan from A grobacterium sp. ZX09. *Carbohydrate Polymers*, *82*, 623–628.

Xiu, A., Zhan, Y., Zhou, M., Zhu, B., Wang, S., Jia, A., et al. (2011). Results of a 90-day safety assessment study in mice fed a glucan produced by Agrobacterium sp. ZX09. *Food and Chemical Toxicology*, *49*, 2377–2384.

Xiu, A., Zhou, M., Zhu, B., Wang, S., & Zhang, J. (2011). Rheological properties of Salecan as a new source of thickening agent. *Food Hydrocolloids*, *25*(7), 1719–1725.

Yildiz, B., Isik, B., & Kis, M. (2002). Thermoresponsive poly(N-isopropylacrylamide-co-acrylamide-co-2-hydroxyethyl methacrylate) hydrogels. *Reactive and Functional Polymers*, *52*, 3–10.

Yu, L., & Ding, J. (2008). Injectable hydrogels as unique biomedical materials. *Chemical Society Reviews*, *37*, 1473–1481.

Zaharia, C., Tudora, M.-R., Stancu, I.-C., Galateanu, B., Lungu, A., & Cincu, C. (2012). Characterization and deposition behavior of silk hydrogels soaked in simulated body fluid. *Materials Science and Engineering C*, *32*, 945–952.

Zhang, Y., Xia, L., Pang, W., Wang, T., Chen, P., Zhu, B., et al. (2013). A novel soluble β-1,3-D-glucan Salecan reduces adiposity and improves glucose tolerance in high-fat diet-fed mice. *British Journal of Nutrition*, *109*, 254–262.

Zhao, Q., Sun, J. Z., Ling, Q. C., & Zhou, Q. Y. (2009). Synthesis of macroporous thermosensitive hydrogels: a novel method of controlling pore size. *Langmuir*, *25*, 3249–3254.

Zhou, M., Jia, P., Chen, J., Xiu, A., Zhao, Y., Zhan, Y., et al. (2013). Laxative effects of Salecan on normal and two models of experimental constipated mice. *BMC Gastroenterology*, *13*, 52–57.